International Journal of Engineering, Mathematical and Physical Sciences
ISSN: 2517-9934
Vol:11, No:8, 2017

Compact Optical Sensors for Harsh Environments

Branislav Timotijevic, Yves Petremand, Markus Luetzelschwab, Dara Bayat, Laurent Aebi

***Abstract*—**Optical miniaturized sensors with remote readout are required devices for the monitoring in harsh electromagnetic environments. As an example, in turbo and hydro generators, excessively high vibrations of the end-windings can lead to dramatic damages, imposing very high, additional service costs. A significant change of the generator temperature can also be an indicator of the system failure. Continuous monitoring of vibrations, temperature, humidity, and gases is therefore mandatory. The high electromagnetic fields in the generators impose the use of non-conductive devices in order to prevent electromagnetic interferences and to electrically isolate the sensing element to the electronic readout. Metal-free sensors are good candidates for such systems since they are immune to very strong electromagnetic fields and given the fact that they are non-conductive. We have realized miniature optical accelerometer and temperature sensors for a remote sensing of the harsh environments using the common, inexpensive silicon Micro Electro-Mechanical System (MEMS) platform. Both devices show highly linear response. The accelerometer has a deviation within 1% from the linear fit when tested in a range 0 – 40 g. The temperature sensor can provide the measurement accuracy better than 1 °C in a range 20 – 150 °C. The design of other type of sensors for the environments with high electromagnetic interferences has also been discussed.

***Keywords*—**Accelerometer, harsh environment, optical MEMS, pressure sensor, remote sensing, temperature sensor.

I. Introduction

THE environments which are considered as harsh: turbo-generators, tunnel mills-drives, mining sites, nuclear and chemical plants, dams and geotechnical systems require continuous monitoring of vibrations, temperature, pressure, humidity and other environmental factors in order to avoid very high, additional service costs. High electromagnetic fields in some of these systems lead to the development of optical, metal-free sensors due to the fact that they are insensitive to very strong electromagnetic fields [1] and that they are non-conductive. Another great advantage of the optical approach is a possibility for the remote monitoring by using optical fibres for the signal transmission.

The MEMS technology based on silicon is a good match with these optical sensors since it allows for cheap, compact, and robust sensing elements such as accelerometers, inclinometers, and pressure and temperature sensors. In addition, the sensors can often entirely or partially share a common MEMS platform for the microfabrication.

A number of different approaches for accelerometers have been reported [2]. Recent works have mainly explored solutions based on grating filters [3], [4], Fabry-Perot filters [5], and Michelson interferometer [6]. An optical MEMS accelerometer reported here is using a seismic MEMS mirror to split the input light to the output fibres. Regarding the approach for the temperature sensor, even though GaAs has more preferable temperature dependent absorption edge shift since its bandgap energy drops faster with the temperature increase [7], our simulations have indicated that Si as a direct bandgap material can also be used. An optical MEMS temperature sensor presented in this work is based on the absorption dependent transmission in silicon waveguides. There are other types of devices such as inclinometers and pressure sensors, which can also be realized in silicon MEMS by exploiting the Fabry-Perot cavities for example. They have also been briefly addressed in this paper. The technology platform common for all the MEMS devices is following a simple process flow consisting of a standard photolithography, a dry etching and an HF release. The packaged sensors are characterized by measuring the responses to accelerations, temperatures and pressures in ranges 0 – 40 g, 20 – 150 °C and 0 – 5 bars, respectively.

B. Timotijevic, Y. Petremand, M. Luetzelschwab and D. Bayat are with CSEM, Rue Jaquet-Droz 1, Neuchatel, CH-2002, Switzerland (corresponding authors, phone: +41327205111; fax: +41327205740; email: bti@csem.ch).

L. Aebi is with MC-monitoring, Route André Piller 19, Givisiez, CH-1762, Switzerland (phone: +41584115440, email: laurent.aebi@mc-monitoring.com).

II. The Design of Sensors

A. MEMS Accelerometers

The basic elements of the Si accelerometer chip are: a seismic mass, a triangular mirror, damping gel areas, an input fibre, and the output fibres. The movable structures are suspended by springs, which are designed in such a way to allow for the in-plane movement only, redirecting the optical signal from an input fiber into two output fibers. Fig. 1 shows the layout of the chip, where the input fiber and the two output fibers are at 70°.

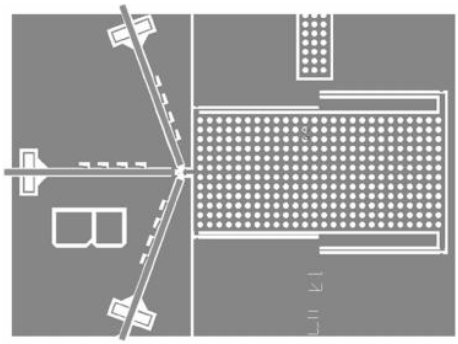

Fig. 1 MEMS optical accelerometer layout

The seismic mass and the springs were optimized to provide sufficiently high resonance frequencies for the specific application. The initial designs had two basic families, one

with the first resonance at 1 kHz, and another one with the first resonance at 3 kHz, which corresponded to the mirror displacement of 10 μm and 1 μm, respectively, at an acceleration of 40 g. The final design has a resonant frequency of 1.7 kHz; this was seen as a good compromise between the resonant frequency and the possible displacement of the structure. To increase the linear frequency range, a damping has been introduced into the MEMS structure.

Operating principle of the device is fairly simple. In absence of the acceleration, the signals in the output fibers are roughly identical. When the mass is subjected to acceleration, the displacement of the mirror induces an increase of optical power in one fiber and a reduction in the other one (Fig. 2). The differential signal from the two output fibers is collected and analyzed in a remote readout module.

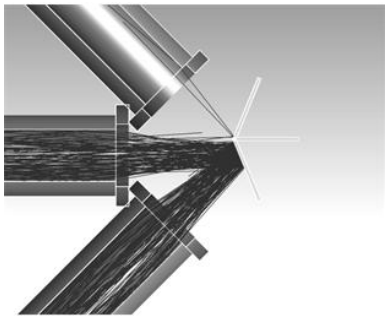

Fig. 2 MEMS accelerometer principle: moving mirror redirects light to one of the output fibres depending on the acceleration level

Zemax ray tracing simulations were performed to optimize the optical power as a function of geometrical parameters. Fig. 3 (a) shows the simulated optical power of the output fibers as a function of the lateral mirror displacement. The acceleration is calculated by substracting these two signals, as shown in Fig. 3 (b). Deviation from linearity is expected to be less than 1% for displacements up to 10 μm for accelerations up to 40 g.

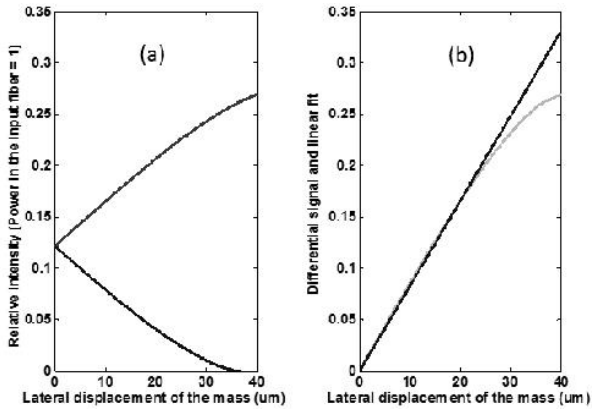

Fig. 3 (a) Simulated signals at the output fibers as a function of the MEMS mirror displacement. (b) Differential signal (grey curve) and its linear fit (black curve)

B. MEMS Temperature Sensor

The basic concept of the temperature sensor is shown in Fig. 4. The light from the input fibre enters the central Si block where it is guided towards the exit fibre. While travelling through the Si waveguide, the light is absorbed. The amount of the absorption depends on the waveguide length, but it also depends on the temperature of the environment [8]; the increase in the temperature enhances the absorption of light, giving the lower optical power at the output. The sensing part contains tapers, integrated lenses and angled corners, designed to maximize the total internal reflection and minimize the losses.

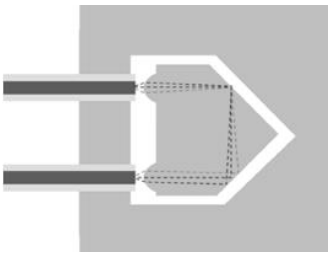

Fig. 4 The concept of the temperature sensor (top down view)

The waveguides are modelled using software simulation tools (Zemax, MATLAB) to make the sensing part long enough to absorb the desired amount of light, but also to shape it properly to prevent other types of losses. These simulations are showing that the optical power reaching the output fibre drops by more than 50% when the temperature increases from 20 °C to 150 °C, indicating a good sensor sensitivity.

C. Other Types of MEMS Sensors for Harsh Environments

Gas sensors, inclinometers, humidity, and pressure sensors are among those which can be realized using very similar MEMS platform as the sensors from the previous two chapters. Inclinometers for example are currently being developed by designing angle dependent Fabry-Perot cavity. MEMS gas sensors could utilize similar structure as the temperature sensor where a gas cell compartment is embedded within a silicon waveguide. Finally, pressure sensor would also rely on the Fabry-Perot structure, where one resonator side (membrane) deflects with the pressure change. In this case, however, the process flow used for the abovementioned sensors needs few more complex adjustments. For this reason, the pressure detection system was as a first step developed using a commercial sensitive element, a mini-spectrometer and an LED (Fig. 5). A MATLAB code is used for the data acquisition and calculation of the Fabry-Perot gap, i.e. pressure. The goal of this demonstrator was to develop the system which would also be compatible with the same strong electromagnetic environments as the previous sensors, but also to demonstrate the precision of the signal acquisition technique of better than 1 part in 6000 (of the used Fabry-Perot cavity), in order to use it later on with the in-house fabricated MEMS pressure sensors.

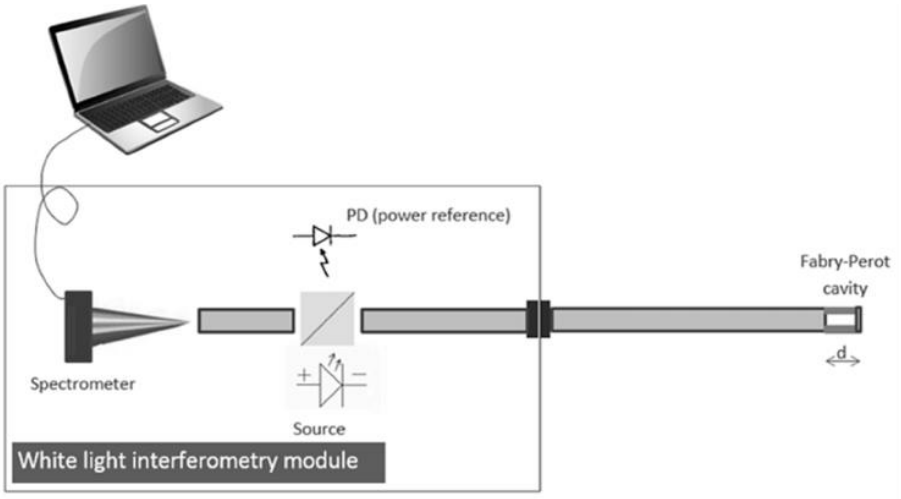

Fig. 5 A concept for an optical pressure sensor

III. Microfabrication and Packaging

As outlined in the previous chapter, the following sensors can be made in a common fabrication process: accelerometers, inclinometers, gas sensors, humidity sensors and temperature sensors. Two sections below provide details for accelerometers and temperature sensors, for which the development has been finished.

A. Microfabrication

Microfabrication has been designed to have two masks and DRIE step on 6" SOI (Silicon-On-Insulator) wafers, where the handle layer, the buried oxide layer and the device layer have thicknesses of 500 µm, 3 µm, and 120 µm, respectively. The structures are defined in the oxide mask by photolithography. After a first partial etching of the handle layer, the device structures are transferred into silicon by DRIE etching through the entire device layer down to the buried oxide. After stripping the remaining photoresist, protecting the obtained structures, finalizing the backside etching and cleaning the wafer, the buried oxide is partially etched to release the movable structures. The release was performed by a timed quasi-dry etching in vapour HF, where the oxide needs to be sufficiently etched to release the movable structure, but on the other side, the oxide must not be over-etched to maintain the oxide which serves as a support for the non-moving parts of the device layer. Surface treatments have been used to polish the lateral surfaces as a way of optimizing the mirror reflectivity. After mechanical separation of the chips, the process continues at chip level: at this point the chip is ready for the assembly with the optical fibers in the package. Fig. 6 shows fabricated sample of a temperature chip.

B. Assembly

The first level package provides a base for the interface between the MEMS device and the optical fibers, but also as a protective housing for the second level package. Because of the strong electromagnetic fields in some of the target applications, all available packaging materials containing metal were excluded. Additionally, temperatures up to 150 °C and a hydrogen rich atmosphere (5 bars) represent further constraints in the choice of the packaging material. Since the target applications for the sensors do not require hermetic sealing, PEEK material was chosen because of its good chemical and physical properties, as well as its adequate machinability.

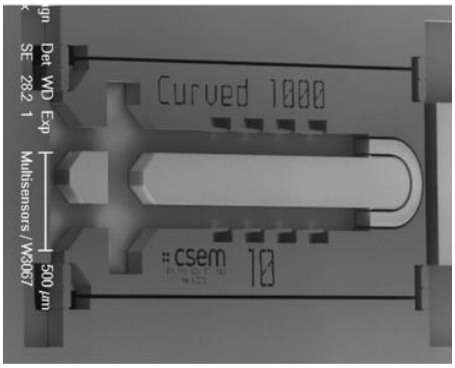

Fig. 6 SEM image of the temperature sensor chip

Fig. 7 shows an assembly of the fibre on the Si temperature chip. The optical fibers are completely moulded in the adhesive, which is UV cured to provide an effective strain relief. Otherwise, the fibres would exert a detrimental force on the chip during handling and the device operation. For the temperature sensor, the input and the output fibers are placed in parallel whereas for the accelerometer sensor the output fibers are placed at an angle of α (70° or 45°) with respect to the central input fiber. A six-axis alignment stage (F-206 from PI) with an arbitrary pivot point was used to perform the fibre alignment. Fiber alignment features have been added to the chip to facilitate the fiber insertion. In addition, an angled insertion was applied to slide the fibers into the fibre channels on the MEMS chip. The PEEK support itself features channels for the guidance of the fibers. The outer two channels are curved to reduce the lateral size of the package, but the

minimal bending radii specified by the fibre manufacturers have been respected in order to reduce the bending losses to an acceptable level (0.3-0.4 dB). A glass lid has been added as a mechanical protection for the fibres and the chip. It also reduces the possibility of the optical signal degradation due to the contamination, humidity, and other environmental factors. Fig. 8 shows the fully assembled accelerometer device with connected fibers ready for the characterization.

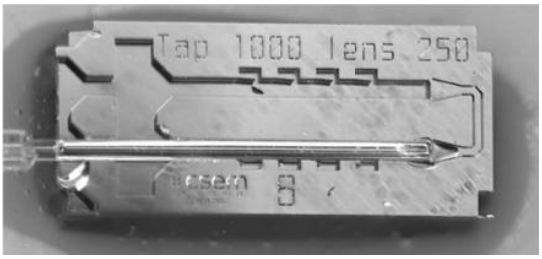

Fig. 7 Assembly of an input fibre with the temperature Si chip

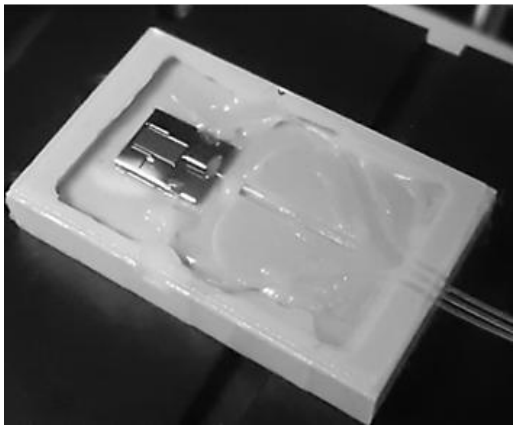

Fig. 8 Assembled accelerometer chip with the fibres

IV. Characterization and Results

A. MEMS Accelerometer

To characterize the sensing performance of the developed accelerometer sensor, the following experimental equipment was used: a function generator, a power amplifier, a shaker, a reference piezo sensor with its charge amplifier and the tested device. With this setup, the frequency response and the dynamic range of five sensors have been obtained. The averaged frequency response of five sensors is plotted in Fig. 9. The frequency response measurement was performed with the electrical readout which has an integrated electrical bandpass filter of 5 Hz to 1000 Hz. Between 20 Hz and 900 Hz, the linearity remains within +/-5%. Outside of this range, the electrical filters are attenuating the mechanical signals, however, in terms of linearity, this fulfils the standards set for certain applications such as the end-winding monitoring for example.

The dynamic range at 100 Hz is plotted in Fig. 10. Excellent dynamic linearity below 1% deviation is obtained up to 13 g. Higher acceleration amplitudes are not reported here due to the given setup limitations, but the values up to 40 g have been verified experimentally at the client's site.

B. MEMS Temperature Sensor

The temperature sensor was characterized in the furnace where the temperature was controlled in a range 30 °C – 150 °C. The measurements were monitored using Thorlabs TSP01 temperature sensor with the accuracy of 0.1 °C. The spectrum analyzer Agilent 86142B was used to measure the optical signals coming from the sensor. The light source in the test setup was the halogen lamp, but only the wavelength range 1.09 µm – 1.13 µm was measured by the spectrum analyzer since the LED source with the central wavelength at 1.11 µm will be used in the final packaged device. Additional level of control was a spectrum taken directly from the white light source using Ocean Optics STS-NIR spectrometer; in order to account for possible oscillations of the source output power, the signal measured by the spectrum analyzer was averaged by the power obtained from the spectrometer.

Typical response of the optical temperature sensor is shown in Fig. 11. The deviation from the linear fit is within 1 °C, whereas if the fit to the 5^{th} order polynomial is used, the error is within 0.8 °C and it can be even further improved by removing the thermal oscillations from the setup and through the thermal passivation (accelerated aging) of the chip before its characterization. The chips were also subject to the thermal cycling at four different fixed temperatures between 20 °C and 150 °C and have confirmed the sensor precision within 1 °C.

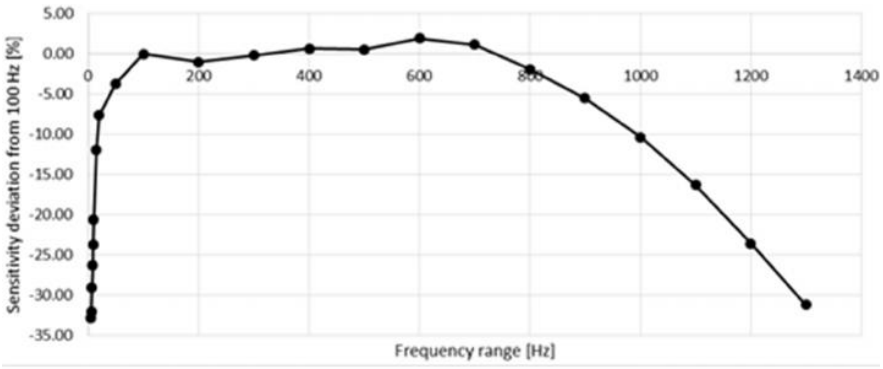

Fig. 9 Averaged frequency response of five specific optical MEMS accelerometers

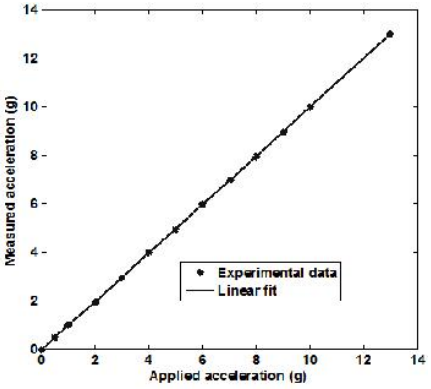

Fig. 10 Performance of one specific optical MEMS accelerometer

C. Pressure Sensor

By using the raw spectrum obtained from the integrated mini spectrometer (setup in Fig. 5) and the developed MATLAB programme, the gap of the commercial Fabry-Perot sensor is estimated to be 17.488 μm at the atmospheric pressure. This is identical to the value provided by the sensor manufacturer. The same method was used to measure and calculate the gap at different chamber pressures in a range 0 – 5 bars. The typical example of the curve gap vs. pressure obtained after several cycles is shown in Fig. 12.

The graph indicates a very good linearity of the sensor with R^2 value of 0.9999 and the sensitivity of ~5.3 nm/mbar. This value was confirmed in the repeated measurements, confirming good reproducibility of the results. The only value that deviated from the linear fit was the value at 0 bar and it was excluded from the fit. The problem with setting up the pressure value around 0 bar was the most likely reason. The error calculated from the linear fit is within +/- 40 mbar range. It should be noted that this is probably not the ultimate performance of the sensor considering that only rough steps of 0.5 bar could be used when setting up the reference chamber pressure (Fig. 12). Similarly, the assessment of the limits (precision) of the data acquisition and analysis requires much better control of the reference pressure. The next step for these devices is a design of a pressure sensor based on the MEMS platform similar to the one reported here and its integration with the source (LED) and mini-spectrometer.

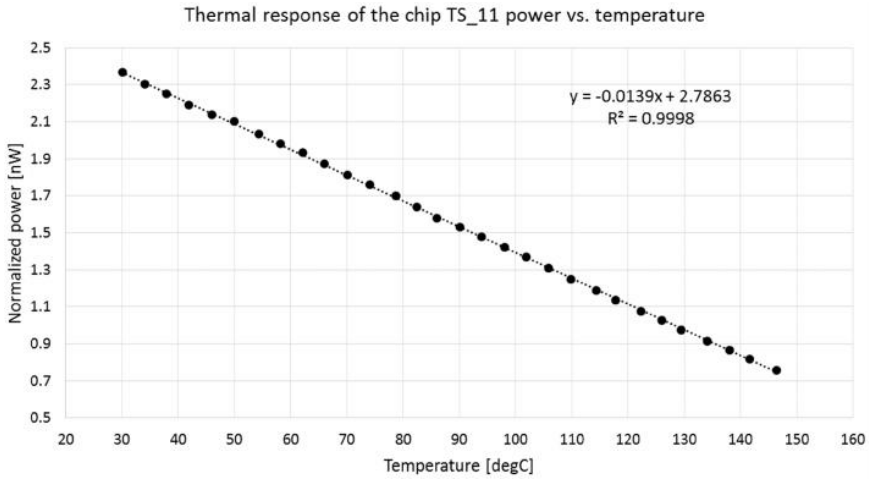

Fig. 11 Performance of one specific optical MEMS temperature sensor

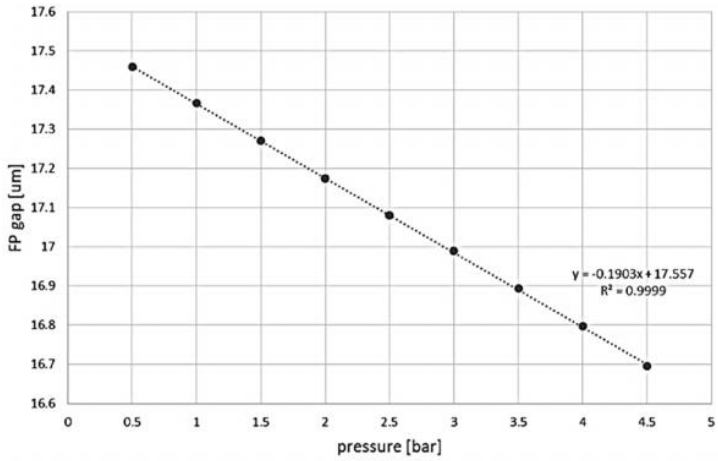

Fig. 12 Fabry-Perrot gap vs chamber pressure

V. Conclusion

We have realized miniature optical accelerometers and temperature sensors for a remote sensing of the harsh environments with strong electromagnetic interferences using the common, inexpensive silicon MEMS platform. Both chips show highly linear response. The accelerometer has a linear error better than 1% in a range 0 – 40 g. The temperature sensor has precision better than 1 °C in a range 20 – 150 °C. We have also developed an optically based pressure demonstrator for a range 0 – 5 bars, which is suitable for the same strong electromagnetic environments, providing precision better than 40 mbar in the given pressure range.

References

[1] D. A. Krohn, T. W. MacDougall, and A. Mendez, "Fiber Optic Sensors: Fundamentals and Applications," SPIE, 2015.
[2] B. Guldimann, "Micromachined fiber optic accelerometer based on intensity modulation", PhD thesis, University of Neuchatel, 2001.
[3] L. Chongyu, H. Luo, S. Xiong, and H. Li, "Investigation of a fiber optic accelerometer based on FBG-FP interferometer," Proc. SPIE 9297, 2014.
[4] Y-G. Lee, D-H. Kim, and C-G. Kim, "Performance of a single reflective grating-based fiber optic accelerometer" Measurement Science and Technology, vol. 23, no. 4, 2012.
[5] Z-Z. Yang, H. Luo, and S-D. Xiong, "High sensitivity fiber optic accelerometer based on folding F-P cavity," Proc. SPIE 8914, International Symposium on Photoelectronic Detection and Imaging: Fiber Optic Sensors and Optical Coherence Tomography, 2013.
[6] F. Peng, J. Yang, B. Wu, Y. Yuan, X. Li, A. Zhou, and L. Yuan, "Compact fiber optic accelerometer," Chin. Opt. Lett. vol. 10, no. 1, 2012.
[7] M. F. Sultan, M. J. O'Rourke, "Temperature sensing by band gap optics absorption in semiconductors," Proc. SPIE 2839, pp. 191-202, 1996.
[8] Y. Zhao, M. Rong, and Y. B. Liao, "Fiber optic temperature sensor used for oil well based on semiconductor optical absorption," IEEE Sensors Journal, vol. 3, no. 4, pp. 400-403, 2003.